doi:10.4149/neo_2022_220206N138

CDC Like Kinase 2 plays an oncogenic role in colorectal cancer via modulating the Wnt/β-catenin signaling

Hai-Bo ZHOU[1,2], Li YANG[3], Shi-Fang LIU[2], Xin-Hua XU[2], Zhuo CHEN[2], Yun-Xiao LI[2], Jin-Hua YUAN[2,*], Yong-Chang WEI[1,*]

[1]Department of Radiation and Medical Oncology, Zhongnan Hospital, Wuhan University, Wuhan, China; [2]Department of Oncology, Yichang Central People's Hospital, China Three Gorges University, Yichang, China; [3]Department of Thyroid and Breast, Yichang Central People's Hospital, China Three Gorges University, Yichang, China

**Correspondence: weiyongchang@whu.edu.cn; xhua1129@126.com*

Received February 6, 2022 / Accepted March 7, 2022

Colorectal cancer (CRC) is a common malignant tumor with high morbidity and mortality, and significant heterogeneity among patients. In this study, we aimed to explore the role and mechanism of CLK2 in CRC, a kinase that phosphorylates SR proteins involved in splicing. Based on the analysis from The Cancer Genome Atlas (TCGA) dataset and tissue microarray, we found that CLK2 was upregulated in CRC tissues and associated with a higher tumor stage and poorer overall survival. Consistent with the bioinformatics analysis, the functional experiments validated that CLK2 acted as a tumor-promoting factor in CRC progression. CLK2 knockdown suppressed aggressive cell proliferation, migration, and invasion *in vitro*, as well as restrained tumor growth *in vivo*. In terms of mechanism, we found that the Wnt/β-catenin signaling pathway was responsible for the CLK2-induced CRC progression, based on the results of pathway enrichment analysis and subsequent experimental validation. Thus, our study, for the first time, identified the role of CLK2 in CRC development and provided a compelling biomarker for targeted therapy in CRC treatment.

Key words: CLK2; Wnt; β-catenin; prognosis; colorectal cancer

Colorectal cancer (CRC) is the third most common malignancy and the fourth leading cause of cancer-related death worldwide [1, 2]. In recent years, the incidence of colorectal cancer in China has increased significantly, with urban incidence ranking second among all cancers [3]. Most CRC patients are diagnosed at late stages due to the absence of early typical clinical symptoms [4]. Despite improvements in surgery and targeted therapy, for advanced patients, there are limited treatment options [5]. One important reason is that the pathogenesis of CRC has not been fully elucidated.

CDC Like Kinase 2 (CLK2) is known as a dual-specificity serine-threonine and tyrosine kinase, which phosphorylates the domain of SR protein to regulate the selective splicing of RNA [6, 7]. CLK2 is involved in multiple biological processes, including homocysteine regulation, neuronal development, cell cycle progression, etc. [8–11]. Meanwhile, the role of CLK2 in tumorigenesis has also been increasingly reported. CLK2 is found to acts as an oncogene in breast cancer and modulate epithelial-to-mesenchymal transition (EMT) splicing patterns [12]. In glioblastoma, CLK2 is found to play a critical role in controlling the cell cycle and survival via FOXO3a/p27 pathway [13]. However, to date, there are few reports about CLK2 in CRC, and the expression of CLK2 in CRC and its relationship with prognosis remain unclear.

Abnormal activation of the Wnt signaling pathway leads to atypical cell proliferation and adenoma formation, which is one of the important causes of colorectal cancer [14–16]. In the process of cell carcinogenesis, β-catenin is activated by the Wnt signaling pathway to transfer from the cytoplasm to the nucleus and binds to members of TCF4 (T cytokine) and LEF-1 (lymphoid enhancer factor) to become a central mediator of transcription, leading to tumor formation and progression [17, 18]. Exploring the regulatory factors of the Wnt /β-catenin pathway can provide more evidence for targeted therapy of colorectal cancer.

In this study, for the first time, we found that CLK2 is highly expressed in CRC and associated with a poor prognosis of CRC patients. The *in vitro* data demonstrated that CLK2 promoted cell proliferation, migration, and invasion. Pathway Enrichment Analysis unfolded that the Wnt/β-catenin signaling was activated in high CLK2 patients, which is validated by *in vivo* and *in vitro* experiments, suggesting it may be potential mechanisms responsible for CLK2-mediated malignant phenotypes. Overall,

our data identify the carcinogenic role of CLK2 in the development of CRC, which may provide a novel target in CRC treatment.

Materials and methods

Bioinformatic analysis. The Tumor Immune Estimation Resource (TIMER) database containing 10,897 samples from The Cancer Genome Atlas (TCGA) (https://cistrome.shinyapps.io/timer/) was applied to pan-cancer expression analysis. CRC microarray data were obtained from the GEO database, including GSE39582 (Platform: GPL510), GSE21510 (Platform: GPL570), GSE25070 (Platform: GPL6883), and GSE41258 (Platform: GPL96). The extracted data were normalized and processed by log2 transformation. The microarray data were normalized with the preprocess Core package in R software (version 3.4.1). The Kaplan-Meier survival analysis with log-rank test was used to compare the survival difference, of which the data was obtained from TCGA dataset. Univariate and multivariate cox regression analysis was performed to identify the risk factors to build the nomogram. The forest was used to show the HR, 95% CI, and p-value of each variable through the 'forestplot' R package. To establish the expression and location of CLK2 in the normal colorectum and CRC tissues, CLK2-related information was searched in The Human Protein Atlas (HPA).

Pathway enrichment analysis. CRC patients from TCGA dataset were categorized into two groups by setting the median mRNA level of CLK2 as a cut-off. The HALLMARK gene set was obtained from the MSigDB database V7.2. GSEA software (v4.0.3) was used to explore the potential biological pathways involved in CRC pathogenesis. The enrichment pathway was classified via the standardized enrichment score (NES). Gene set variation analysis (GSVA) was performed by an unmonitored gene enrichment method to measure changes in pathway activity in an unsupervised manner with the R software (version 3.4.1).

Cell culture. Human CRC cell lines (HT29, SW480, HCT-116, LoVo) were obtained from the Cell Bank of the Chinese Academy of Sciences (Shanghai, China). Cells were cultured in Dulbecco's Modified Eagle's Medium (DMEM, Invitrogen, Carlsbad, CA, USA) containing 10% fetal bovine serum (FBS, Gibco, Carlsbad, CA, USA) with 100 U/ml penicillin and 100 μg/ml streptomycin (Gibco) at 37 °C in 5% CO_2.

Plasmid construction and cell transfection. The cDNA of CLK2 was amplified from LoVo cells and cloned into pCMV-Tag-Flag2B (Invitrogen) to generate a pCMV-CLK2 plasmid. The target shRNA sequences of CLK2 were synthesized and cloned into pLKO.1-TRC (Invitrogen) to generate pLKO.1-shCLK2#1 and pLKO.1-shCLK2#2 plasmids. Cells were transfected using Lipofectamine 2000 (Thermo Fisher Scientific, USA) according to the product manual. CRC cells were infected with lentivirus in the presence of polybrene (5 ng/ml) to generate stably infected cells.

Cell counting kit-8 (CCK-8) assay. The cell counting kit-8 (CCK-8) assay (Sigma, St. Louis, MO, USA) was performed according to the manufacturer's instructions. Cells were plated in 96-well plates at a density of 1×10^3 cells/well. CCK-8 assay was performed every 24 h. In brief, 10 μl of CCK-8 solution was added to each well, and the cells were incubated with the solution for another 1 h. Optical density (OD) values were measured at 450 nm using a microplate reader (Potenov, Beijing, China) to indicate the relative cell viability.

Colony formation assay. Cells were seeded in a 6-well plate at a density of 1×10^3 cells/well and maintained for 14 days. Then cells were fixed for 15 min in 4% paraformaldehyde and stained with 1% crystal violet for 1 min. After washing with PBS extensively, colonies were photographed and counted.

5-Ethynyl-2'-deoxyuridine (EdU) assay. EdU assay was performed with the usage of an EdU kit (RiboBio, Guangzhou, China). Cells were co-cultured with EdU working solution (1:1000) at 37 °C in a humidified 5% CO_2 atmosphere for 2 h, followed by fixation with 4% paraformaldehyde for 30 min and treatment with 0.5% Triton X-100 for 30 min. Then cells were co-incubated with click reaction solution for 30 min at room temperature in a dark environment, after which cells were treated with Hoechst solution for 10 min. Stained cells were captured under an inverted microscope (Olympus, IX51, Japan) at ×200 magnification. Cell counting was conducted by ImageJ 1.8.0v.

Transwell assay. Cell migration and invasion assays were detected with Transwell chambers (Corning, NY, USA). In cell migration assay, 5×10^5 cells were suspended in a serum-free medium and transferred into the upper chamber of each Transwell plate, while the bottom chamber was filled with 800 μl 20% FBS DMEM as a chemoattractant. After the culture for 24 h, cells in the upper surface were removed with cotton swabs, and cells remaining on the bottom surface were fixed with 4% methanol at room temperature for 15 min, followed by staining with 1% crystal violet (Sangon Biotech, Shanghai, China) for 20 min at room temperature. Stained cells were captured under an inverted microscope at ×200 magnification, and the number of migrated cells of five randomly selected fields was counted using ImageJ 1.8.0v. In cell invasion assay, the filter was pre-coated with diluted Matrigel (BD Biosciences, Sparks, MD), and the other procedures were executed as described above.

Luciferase reporter assay. Cells were seeded on 96-well plates at a density of 4×10^3 cells/well. TOPFlash or FOPFlash plasmids were co-transfected with indicated functional plasmids into cells for 36 h. Luciferase activity was measured with the Dual Luciferase Assay Kit (Promega, Madison, WI, USA). The firefly luciferase activity level was normalized to Renilla luciferase. The fold-increase indicating the TOPFlash activity compared to the FOPFlash is reported.

Immunofluorescence staining. Cultured cells were fixed in 4% paraformaldehyde, permeabilized in 0.2% Triton X-100, and primary antibody against β-catenin (sc-7963,

Santa Cruz) was applied, followed by the incubation with FITC-conjugated goat antibody (#405305, Biolegend). Images were acquired using an Olympus IX71.

Western blotting. The RIPA lysis buffer (ASPEN) was used to lyse the CRC cell lines and tissues. Then, proteins were collected and quantified using the bicinchoninic acid (BCA) kit (ASPEN). 40 μg of protein per lane was isolated via 10% SDS-PAGE and then transferred onto a PVDF membrane (Millipore, Schwalbach, Germany). After being blocked with 5% skimmed milk in TBST (Tris-Buffered Saline Tween-20), membranes were incubated with specific antibodies against human CLK2 antibody (1:1000, ab188141, Abcam, Cambridge, UK), β-Catenin antibody (1:3000, CST, #8480), and GAPDH antibody (1:10000; ab181602, Abcam, Cambridge, UK).

Real-Time PCR assay. Total RNA was isolated by TRIzol reagent (Vazyme, China) and reverse transcribed into complementary DNA (cDNA) using the M-MLV reverse transcriptase (Vazyme). qRT-PCR was performed on the ABI 7500 Fast Real-Time PCR System (Applied Biosystems, Waltham, MA, USA) using SYBR Green PCR kit (Vazyme). Relative gene expression levels were calculated by $2^{-\Delta\Delta Ct}$. GAPDH was used as an endogenous control. Primers used for RT-PCR are listed in Supplementary Table S1.

Tumor xenograft model. All experiments were conducted according to the Guidelines and approved by The Institutional Animal Care and Use Committee at The First College of Clinical Medical Science, Three Gorges University. 4-week-old male BALB/c-nude mice (Shanghai SLAC Laboratory Animal Co., Ltd.) were randomly divided into four groups (n=8 per group). Infected cells (5×10^6 per injection) were inoculated into the right and left flanks of the mice via subcutaneous injection. Tumor volume was measured every 3 days and calculated with the following formula: Volume = (length×width^2)/2. After 30 days, all mice were sacrificed and subcutaneous tumors were excised and further analyzed.

Statistical analysis. The data are presented as the mean ± SD (standard deviation) of at least three independent experiments. Data analysis was performed using the SPSS 25.0 software and GraphPad Prism 8.0. Significant differences between the two groups were evaluated by Student's t-tests, and one-way ANOVA. Relationships between protein expression levels and clinicopathological information were assessed by Chi-square or Fisher's exact tests. The survival curve was generated using the Kaplan-Meier method, and differences were estimated by the log-rank test. Pearson's correlation coefficient was used for statistical correlation analysis. A p-value <0.05 was considered statistically significant.

Results

The expression level of CLK2 is increased in CRC patients. To evaluate the clinical significance of CLK2 in CRC, we examined the expression of CLK2 in CRC. The results from the TIMER database indicated that CLK2 was highly expressed in 15 tumors, including colon and rectal cancer (Figure 1A). In addition, CLK2 was highly expressed in CRC in GSE39582, GSE21510, and GSE25070 (Figures 1B–1D). Compared with normal tissues, the expression level of CLK2 in polyp and colon primary cancer was successively increased. Meanwhile, the expression level in liver metastasis tissues was significantly higher than that in primary cancer and normal liver tissues, as well as the expression in lung metastasis (Figures 1E–1G). To further assess the expression of CLK2 at the protein level, we analyzed the IHC results from the Human Protein Atlas (HPA) and found that CLK2 IHC staining was remarkably higher in CRC tumors than in the normal colon and normal rectum tissues (Figure 1H). Moreover, we detected the expression of CLK2 in 14 matched CRC and adjacent normal tissues from mRNA and protein levels and confirmed the expression pattern (Figures 3A, 3B). Taken together, these data reveal that CLK2 is highly expressed in CRC and may be involved in multiple stages of CRC occurrence and development.

High CLK2 level indicates a poor prognosis of CRC patients. To evaluate CLK2 in predicting the prognosis of CRC patients, the association between CLK2 expression and the overall survival (OS) and the progression-free survival (PFS) were analyzed in TCGA cohort. The patients with higher expression of CLK2 had poorer OS and PFS (Figures 2A, 2B). Univariate Cox regression analysis revealed CLK2 expression acted as an independent prognostic factor for poor survival (Figures 2C), and approximately an independent prognostic factor by multivariate Cox regression

Table 1. Correlation between clinicopathological variables and CLK2 expression of CRC patients in TCGA.

	CLK2 high (n=310)	CLK2 low (n=310)	p-value
Age	66.9 (12.8)	65.7 (12.8)	0.270
Gender			0.376
Female	151	139	
Male	159	171	
T stage			0.048
Tis, T1, T2	53	73	
T3, T4	256	237	
N stage			0.057
N0	164	188	
N1, N2, NX	145	122	
M stage			0.413
M0	224	235	
M1, MX	80	72	
TNM stage			0.033
I	45	60	
II	109	119	
III	98	81	
IV	48	40	
Neoadjuvant			0.124
No	310	306	
Yes	0	4	

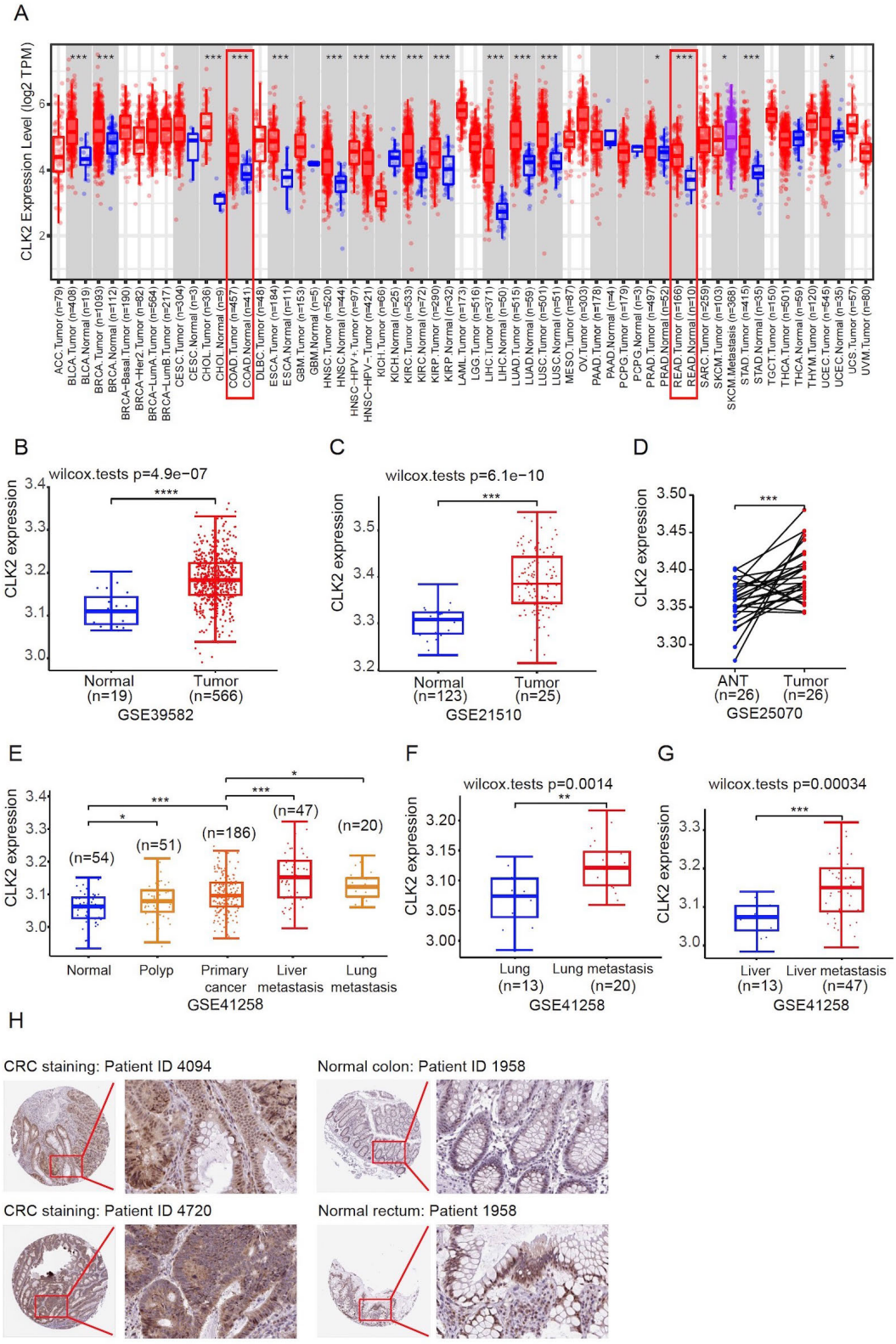

Figure 1. Bioinformatics analysis of CLK2 expression level. A) Pan-Cancer Analysis of CLK2 expression in tumor and normal tissues from TIMER database. B–D) CLK2 expression in tumor and normal tissues in CRC from GSE39582, GSE21510, GSE25070, respectively. E–G) CLK2 expression in normal, polyp, primary tumor, liver metastasis, lung metastasis tissues from GSE41258. H) Representative immunohistochemical staining in CRC, normal colon, and normal rectum tissues from the Human Protein Atlas (HPA). *p<0.05; **p<0.01; ***p<0.001.

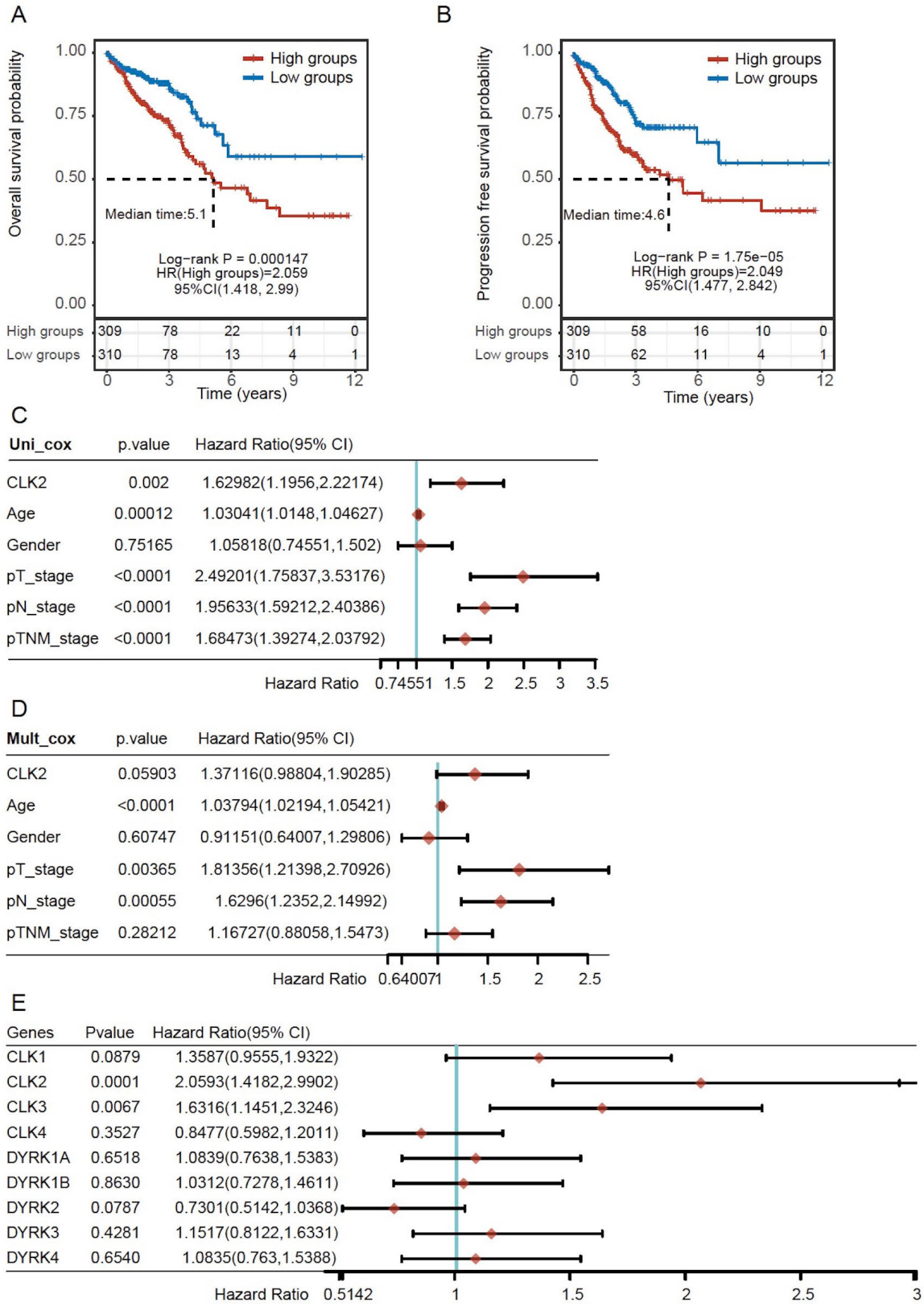

Figure 2. Relationship of CLK2 level and prognosis of CRC patients. The correlation between CLK2 expression and OS (A) and PFS (B). Hazard ratio and p-value of constituents involved in the univariable (C) and multivariate Cox regression (E). Hazard ratio and p-value of DYRKs and CLKs.

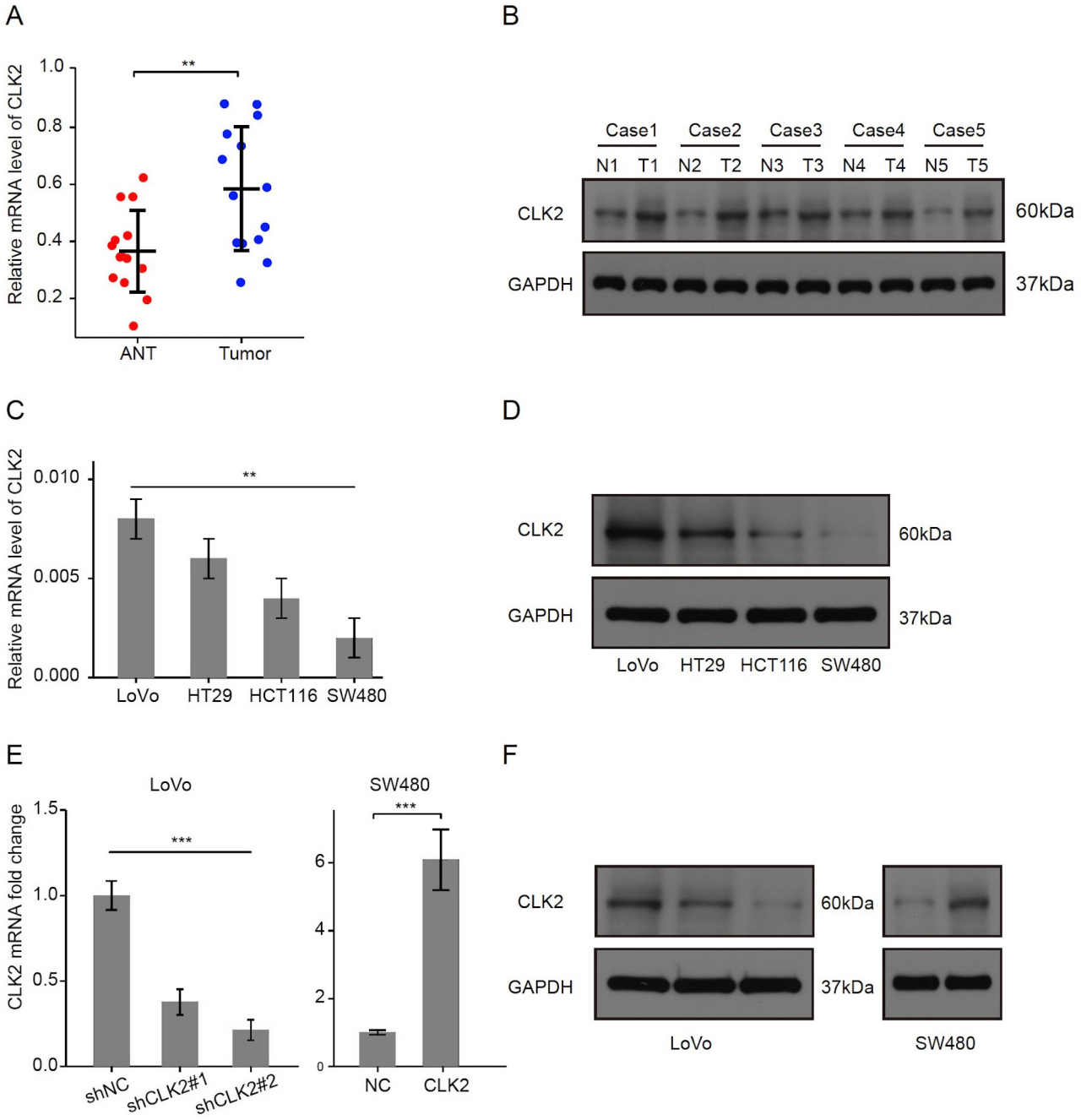

Figure 3. Expression of CLK2 in CRC patients and cell lines. A) mRNA levels of CLK2 in CRC tissues and adjacent normal tissues. B) Protein levels of CLK2 in CRC tissues and adjacent normal tissues. The mRNA (C) and protein (D) levels of CLK2 in HT-29, HCT116, LoVo, and SW480 cell lines. Stable knockdown of CLK2 in LoVo cells and overexpression in SW480 cells, measured by qPCR (E) and western blot (F). *p<0.05; **p<0.01; ***p<0.001.

analysis (Figures 2D). Additionally, upregulated CLK2 levels were significantly positively correlated with poor TNM stage (Table. 1). The CLK family comprises four members: CLK1-4 and is highly related to the DYRK family, which also consists of four members: DYRK1-4. CLKs and DYRKs belong to a family of 62 serine/threonine kinases known as the CMGC group [6]. We thus examined the prognosis role of DYRKs and CLKs and found that CLK2 was the most significant in predicting survival. Collectively, all these results indicate that CLK2 levels may be used as an independent predictor for prognosis in CRC patients.

CLK2 promotes the malignant phenotypes of CRC cells. To investigate the potential biological function of CLK2, we first detected the CLK2 expression in four

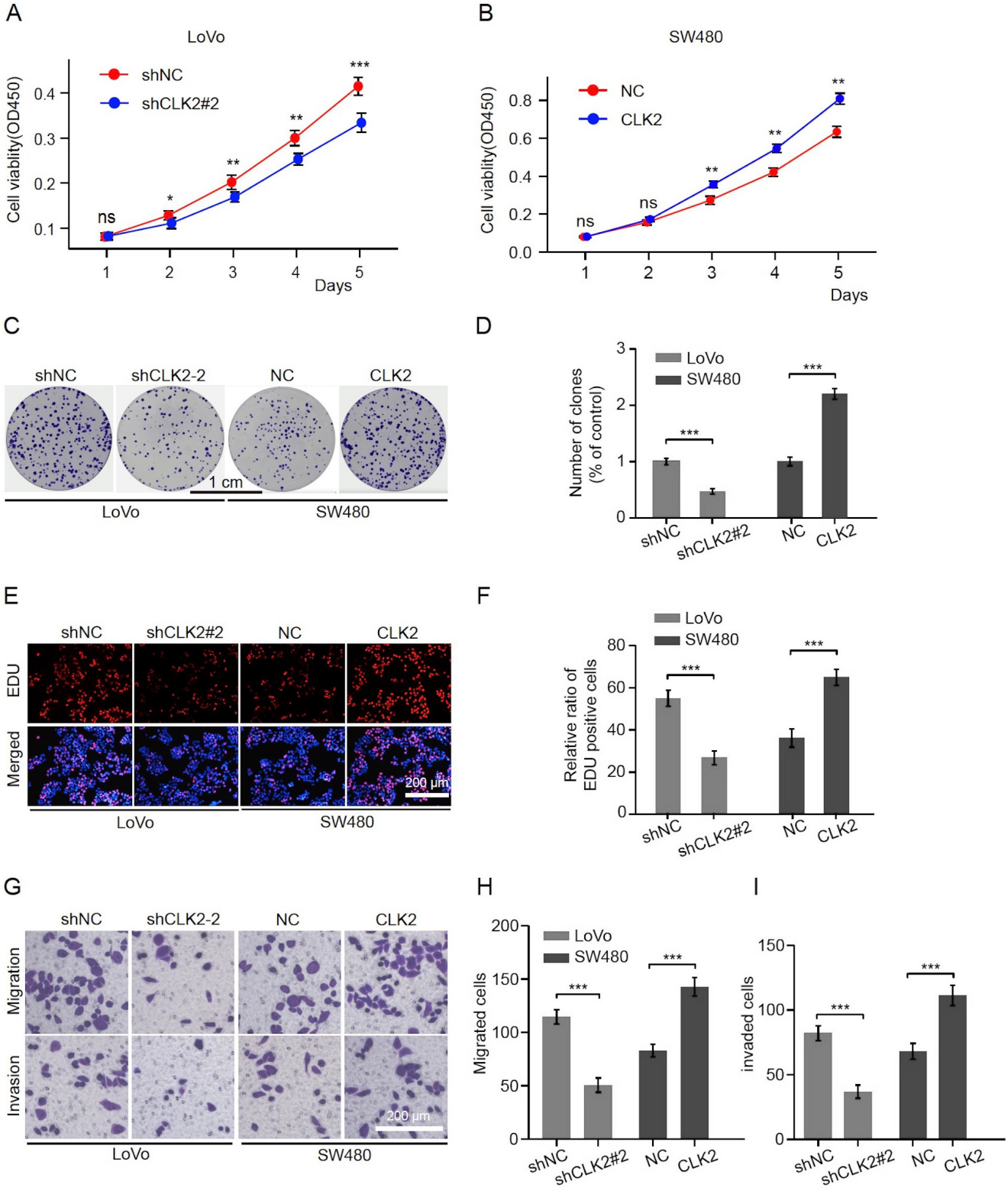

Figure 4. CLK2 promoted the proliferation and metastasis of CRC cells. A) The proliferation capability of LoVo and SW480 cells was detected by CCK-8 (A, B), clone formation (C, D), and EdU assay (E, F). G–I) The migration and invasion capability of LoVo and SW480 cells were monitored by Transwell assay. Scale bars: 200 μm. *p<0.05; **p<0.01; ***p<0.001.

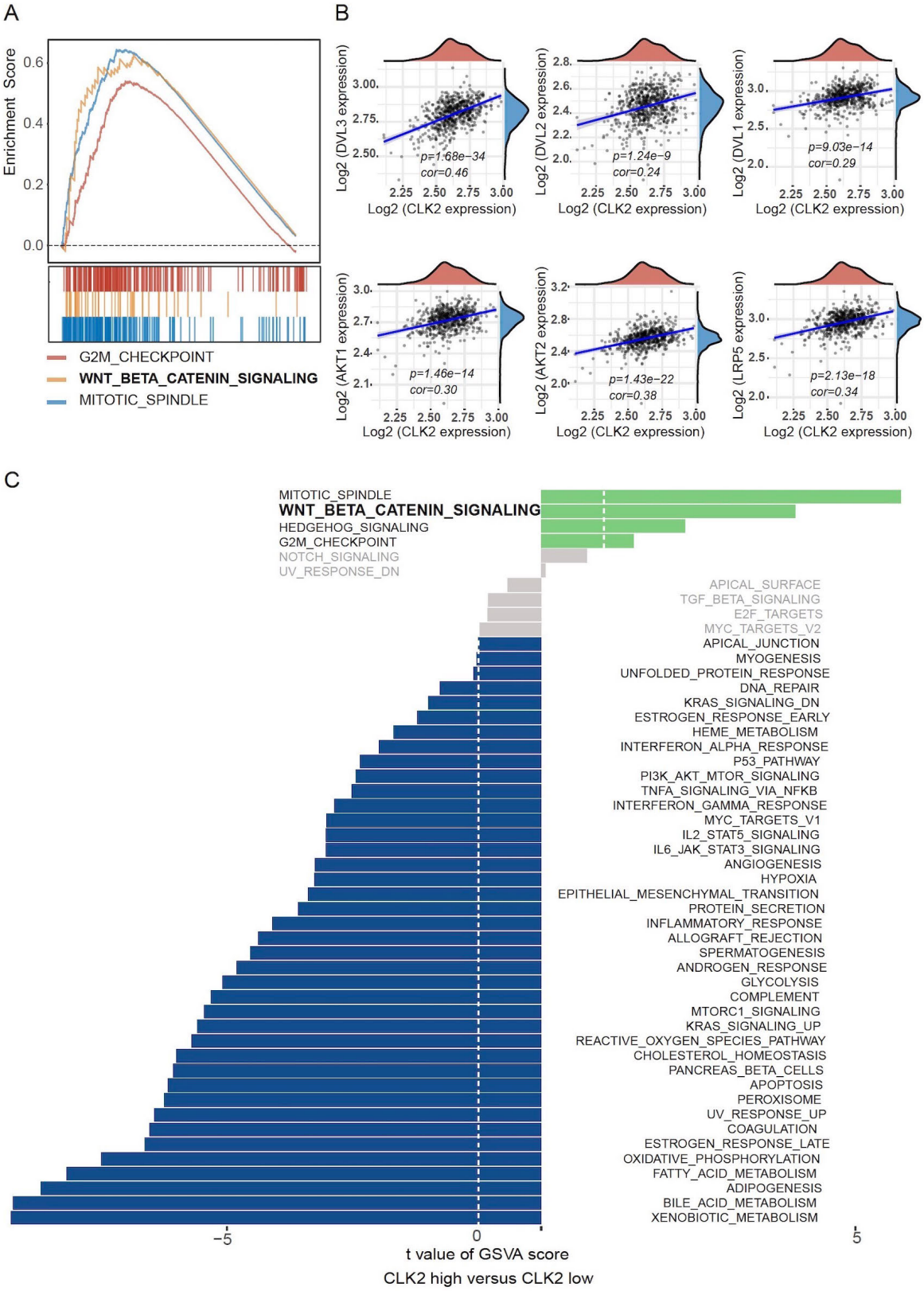

Figure 5. Enrichment plots from GSEA and GSVA. A) GSEA determined hallmark pathways associated with the CLK2 level. B) The correlations of CLK2 with several molecules in the Wnt/β-catenin signaling pathway. C) GSVA determined the hallmark pathway associated with the CLK2 level.

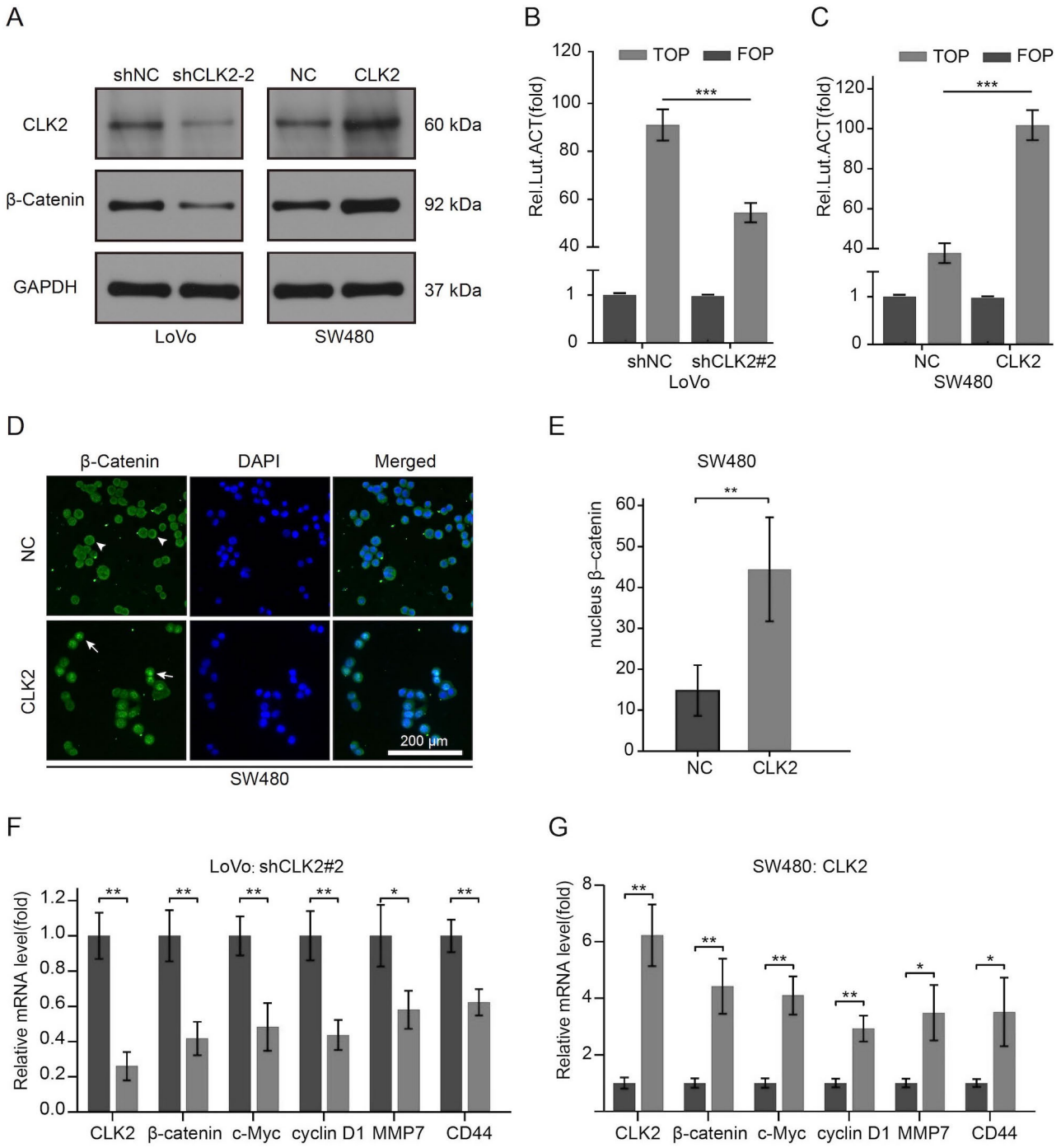

Figure 6. Effect of CLK2 on the Wnt/β-catenin signaling. A) Protein level of β-catenin in CLK2 silenced LoVo cells and CLK2 overexpressed SW480 cells. B, C) TOP/FOP luciferase reporter assays of CLK2 silenced LoVo cells and CLK2 overexpressed SW480 cells. D, E) Immunofluorescent staining of β-catenin in CLK2 overexpressed SW480 cells; scale bars: 200 μm. F, G) The expression of Wnt-related genes in CLK2 silenced LoVo cells and CLK2 overexpressed SW480 cells detected by qRT-PCR. *p<0.05; **p<0.01; ***p<0.001.

CRC cell lines. We found that the expression of CLK2 was relatively high in LoVo cells and low in SW480 cells (Figures 3C, 3D), and these two cell lines were selected for further exploration. Next, we stably silenced CLK2 in LoVo cells and overexpressed CLK2 in SW480 cells, which was validated by qPCR and western blot (Figures 3E, 3F). The CCK-8, colony formation, and EDU assays showed that the reduction of CLK2 significantly suppressed the prolif-

erative capacity of LoVo cells, while the overexpression of CLK2 worked oppositely in SW480 cells (Figures 4A–4F). Metastasis is the critical cause of CRC progression and recurrence. Thus, we detected the metastasis-related effects of CLK2 on CRC cells. The Transwell assays revealed that CLK2 knockdown significantly attenuated the migration and invasion of LoVo cells, while the CLK2 overexpression worked oppositely in SW480 cells (Figures 4G, 4H). Taken together, these results showed that CLK2 plays a role in promoting CRC development.

CLK2 activates the Wnt/β-catenin signaling. To identify the potential mechanisms accounting for CLK2-mediated CRC progression, we classified TCGA CRC patients into two groups according to the median expression level of CLK2, as bait to perform GSEA and GSVA analysis. Both GSEA and GSVA showed that CLK2 expression was positively associ-

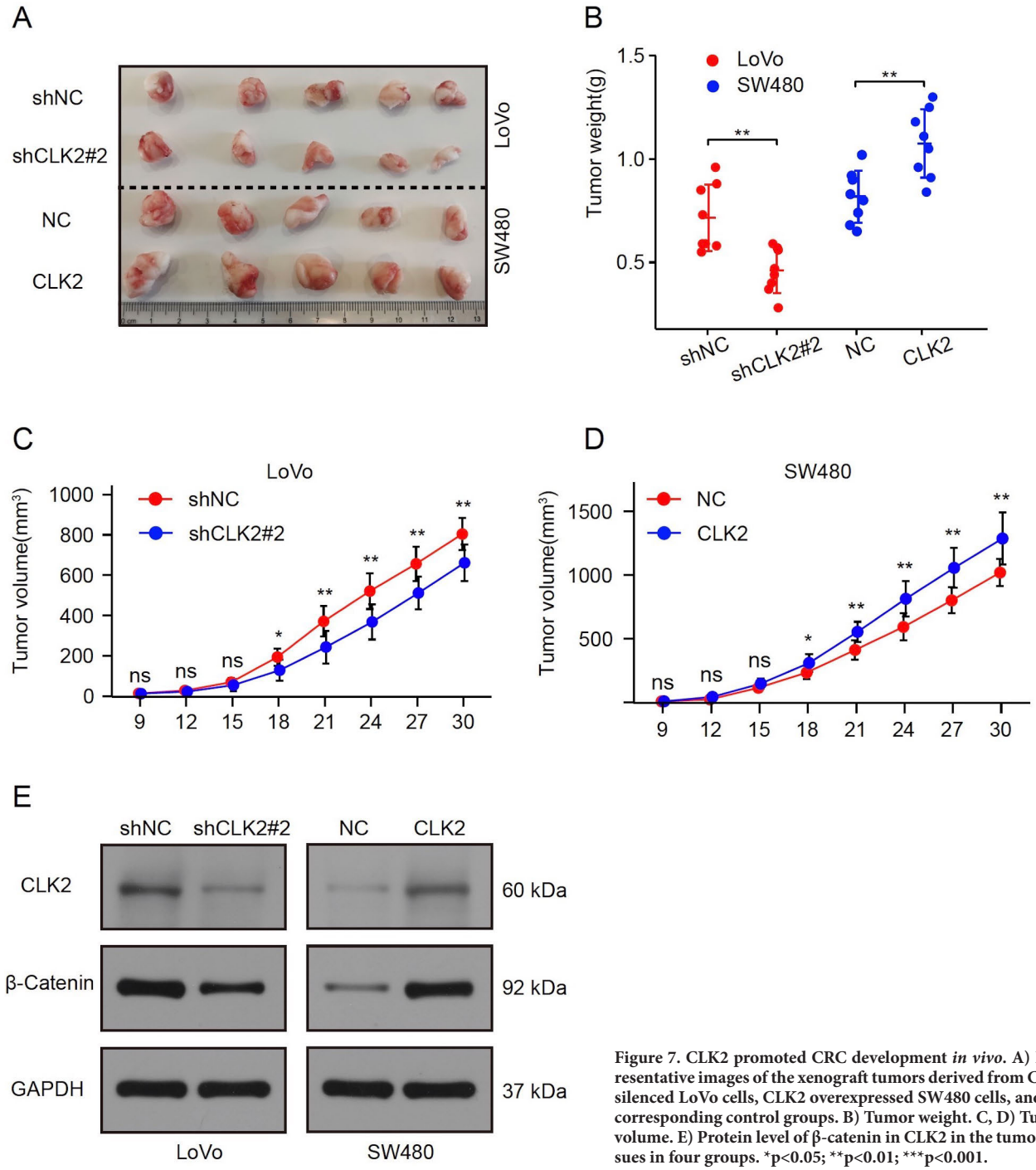

Figure 7. CLK2 promoted CRC development *in vivo*. A) Representative images of the xenograft tumors derived from CLK2 silenced LoVo cells, CLK2 overexpressed SW480 cells, and the corresponding control groups. B) Tumor weight. C, D) Tumor volume. E) Protein level of β-catenin in CLK2 in the tumor tissues in four groups. *p<0.05; **p<0.01; ***p<0.001.

ated with the Wnt/β-catenin signaling, mitotic spindle, and G2/M checkpoint (Figures 5A, 5C). Further investigation demonstrated that several components of the Wnt/β-catenin signaling [19], such as DVL1-3, AKT1, AKT2, and LRP5 were positively correlated with CLK2 (Figure 5B, Supplementary Table S2). To validate the correlation between CLK2 and Wnt/β-catenin signaling, we conducted a TOP/FOP luciferase activity assay and found that CLK2 was a positive regulator of the Wnt/β-catenin signaling (Figures 6B, 5C). The protein level of β-catenin was significantly decreased in CLK2 silenced LoVo cells and increased in CLK2 overexpressed SW480 cells (Figure 6A). Meanwhile, overexpression of CLK2 in SW480 cells promoted the nuclear localization of β-catenin (Figures 6D, 6E). In addition, reduction of CLK2 in LoVo cells resulted in a remarkable decrease in the expression of Wnt/β-catenin related genes including Cyclin D1, CD44, C-myc, and MMP-7 (Figure 6F), whereas overexpression of CLK2 in SW480 cells increased the expression of these genes (Figure 6G). Thus, these results demonstrate that CLK2 activates the Wnt/β-catenin signaling and promotes the nuclear translocation of β-catenin.

CLK2 promotes CRC tumorigenesis *in vivo*. To further verify the oncogenic role of CLK2 in CRC, we performed *in vivo* study. As shown in Figure 7A, silencing of CLK2 could effectively suppress tumor growth, whereas overexpression of CLK2 promoted tumor growth, which was confirmed by tumor weight and tumor size at endpoint (Figures 7B, 7C). Moreover, the protein level of β-catenin was significantly decreased in CLK2 silenced implanted tumors and increased in CLK2 overexpressed implanted tumors, strengthening the important regulation of CLK2 on the Wnt/β-catenin signaling pathway in CRC development.

Discussion

CDC Like Kinase is the first identified dual-specific protein kinase that phosphorylates the tyrosine, serine/threonine residues of substrate proteins [6]. The CLK protein kinase family consists of four subtypes: CLK1, CLK2, CLK3, and CLK4. These four subtypes encode proteins with a highly conserved gene sequence at the C-terminal. CLKs are central to exon recognition in mRNA splicing [7–8]. Accumulating evidence indicates that alternative splicing plays a critical role in cancer progression through abnormal expression or mutation of splicing factors [20–22]. Inhibition of CLKs with shRNA or chemical inhibitors blocked cell proliferation in a variety of cell lines, including breast cancer, lung cancer, kidney cancer, and colorectal cancer [12, 23–26]. In breast cancer, CLK2 is overexpressed and its downregulation suppresses breast cancer cells growth and tumorigenesis *in vivo* by regulating EMT-related changes in alternative splicing patterns [12]. CLK2 may also play an important role in the pathogenesis of triple-negative breast cancer (TNBC) and its inhibitors significantly reduce the malignant phenotypes of TNBC cell lines [27]. In glioblastoma, CLK2 is highly expressed and associated with poor survival. Silencing CLK2 reduces the phosphorylation of FOX03a and the expression of Ki-67, thus demonstrating that CLK2 plays an oncogenic role by regulating FOX03a/P27 [13].

Lorecivivint, a small molecule, was proved to directly inhibited CLK2 and DYRK1A to suppress the Wnt/β-catenin signaling for knee osteoarthritis treatment [28]. In terms of mechanism, CLK2 inhibition induced early chondrogenesis without affecting β-catenin [29], suggesting a novel mechanism for the Wnt pathway inhibition. SM08502, a novel small inhibitor of CDC-like kinase, was shown to inhibit Wnt pathway-related gene expression by reducing serine and arginine rich splicing factor (SRSF) phosphorylation and disrupted spliceosome activity [30].

Another CLKs inhibitor, SM09419, potently suppresses Wnt signaling activity through SRSF6 phosphorylation and cell proliferation in MCL cell lines [31]. Our study found that CLK2 activates the Wnt/β-catenin signaling by promoting nuclear translocation of cytoplasmic β-catenin, which is a canonical manner of Wnt pathway regulation [32]. These studies suggest that CLK2 may regulate Wnt signaling in multiple ways, depending on different biological processes. At the same time, the substrates of CLK2 that link splicing pattern and Wnt/β-catenin signaling remains to be further explored.

In summary, our findings demonstrate that high CLK2 expression strongly correlates aggressive phenotypes and poor prognosis in CRC. CLK2 activates the Wnt/β-catenin pathway and promotes the nuclear translocation of β-catenin. In conclusion, these findings indicate that CLK2/Wnt/β-catenin axis may be a potential therapeutic target for CRC patients.

Supplementary information is available in the online version of the paper.

Acknowledgments: We thank Wanqing Shen from Kindstar Globalgene (Beijing) Technology, Inc., for the constructive comments on the writing of this article.

References

[1] SIEGEL RL, MILLER KD, FUCHS HE, JEMAL A. Cancer Statistics, 2021. CA Cancer J Clin 2021; 71: 7–33. https://doi.org/10.3322/caac.21654

[2] CARTWRIGHT TH. Treatment decisions after diagnosis of metastatic colorectal cancer. Clin Colorectal Cancer 2012; 11: 155–66. https://doi.org/10.1016/j.clcc.2011.11.001

[3] ZHANG L, CAO F, ZHANG G, SHI L, CHEN S et al. Trends in and Predictions of Colorectal Cancer Incidence and Mortality in China From 1990 to 2025. Front Oncol 2019; 9: 98. https://doi.org/10.3389/fonc.2019.00098

[4] DEKKER E, TANIS PJ, VLEUGELS JLA, KASI PM, WALLACE MB. Colorectal cancer. Lancet 2019; 394: 1467–1480. https://doi.org/10.1016/S0140-6736(19)32319-0

[5] SHIOKAWA D, SAKAI H, OHATA H, MIYAZAKI T, KANDA Y et al. Slow-Cycling Cancer Stem Cells Regulate Progression and Chemoresistance in Colon Cancer. Cancer Res 2020; 80: 4451–4464. https://doi.org/10.1158/0008-5472.CAN-20-0378

[6] LINDBERG MF, MEIJER L. Dual-Specificity, Tyrosine Phosphorylation-Regulated Kinases (DYRKs) and cdc2-Like Kinases (CLKs) in Human Disease, an Overview. Int J Mol Sci 2021; 22: 6047. https://doi.org/10.3390/ijms22116047

[7] DUNCAN PI, STOJDL DF, MARIUS RM, SCHEIT KH, BELL JC. The Clk2 and Clk3 dual-specificity protein kinases regulate the intranuclear distribution of SR proteins and influence pre-mRNA splicing. Exp Cell Res 1998; 241: 300–308. https://doi.org/10.1006/excr.1998.4083

[8] JIANG N, BÉNARD CY, KÉBIR H, SHOUBRIDGE EA, HEKIMI S. Human CLK2 links cell cycle progression, apoptosis, and telomere length regulation. J Biol Chem 2003; 278: 21678–21684. https://doi.org/10.1074/jbc.M300286200

[9] GLATZ DC, RUJESCU D, TANG Y, BERENDT FJ, HARTMANN AM et al. The alternative splicing of tau exon 10 and its regulatory proteins CLK2 and TRA2-BETA1 changes in sporadic Alzheimer's disease. J Neurochem 2006; 96: 635–644. https://doi.org/10.1111/j.1471-4159.2005.03552.x

[10] RODGERS JT, VOGEL RO, PUIGSERVER P. Clk2 and B56β mediate insulin-regulated assembly of the PP2A phosphatase holoenzyme complex on Akt. Mol Cell 2011; 41: 471–479. https://doi.org/10.1016/j.molcel.2011.02.007

[11] PETSALAKI E, ZACHOS G. Clks 1, 2 and 4 prevent chromatin breakage by regulating the Aurora B-dependent abscission checkpoint. Nat Commun 2016; 7: 11451. https://doi.org/10.1038/ncomms11451

[12] YOSHIDA T, KIM JH, CARVER K, SU Y, WEREMOWICZ S et al. CLK2 Is an Oncogenic Kinase and Splicing Regulator in Breast Cancer. Cancer Res 2015; 75: 1516–1526. https://doi.org/10.1158/0008-5472.CAN-14-2443

[13] PARK SY, PIAO Y, THOMAS C, FULLER GN, DE GROOT JF. Cdc2-like kinase 2 is a key regulator of the cell cycle via FOXO3a/p27 in glioblastoma. Oncotarget 2016; 7: 26793–26805. https://doi.org/10.18632/oncotarget.8471

[14] SCHATOFF EM, LEACH BI, DOW LE. Wnt Signaling and Colorectal Cancer. Curr Colorectal Cancer Rep 2017; 13: 101–110. https://doi.org/10.1007/s11888-017-0354-9

[15] BASU S, HAASE G, BEN-ZE'EV A. Wnt signaling in cancer stem cells and colon cancer metastasis. F1000Res 2016; 5: F1000 Faculty Rev-699. https://doi.org/10.12688/f1000research.7579.1

[16] ANASTAS JN, MOON RT. WNT signalling pathways as therapeutic targets in cancer. Nat Rev Cancer 2013; 13: 11–26. https://doi.org/10.1038/nrc3419

[17] JEONG WJ, RO EJ, CHOI KY. Interaction between Wnt/β-catenin and RAS-ERK pathways and an anti-cancer strategy via degradations of β-catenin and RAS by targeting the Wnt/β-catenin pathway. NPJ Precis Oncol 2018; 2: 5. https://doi.org/10.1038/s41698-018-0049-y

[18] CHI J, ZHANG H, HU J, SONG Y, LI J et al. AGR3 promotes the stemness of colorectal cancer via modulating Wnt/β-catenin signalling. Cell Signal 2020; 65: 109419. https://doi.org/10.1016/j.cellsig.2019.109419

[19] ZHANG M, SHI J, HUANG Y, LAI L. Expression of canonical WNT/β-CATENIN signaling components in the developing human lung. BMC Dev Biol 2012; 12: 21. https://doi.org/10.1186/1471-213X-12-21

[20] OLTEAN S, BATES DO. Hallmarks of alternative splicing in cancer. Oncogene 2014; 33: 5311–5318. https://doi.org/10.1038/onc.2013.533

[21] EL MARABTI E, YOUNIS I. The Cancer Spliceome: Reprograming of Alternative Splicing in Cancer. Front Mol Biosci 2018; 5: 80. https://doi.org/10.3389/fmolb.2018.00080

[22] BONNAL SC, LÓPEZ-OREJA I, VALCÁRCEL J. Roles and mechanisms of alternative splicing in cancer – implications for care. Nat Rev Clin Oncol 2020; 17: 457–474. https://doi.org/10.1038/s41571-020-0350-x.

[23] MURAI A, EBARA S, SASAKI S, OHASHI T, MIYAZAKI T. Synergistic apoptotic effects in cancer cells by the combination of CLK and Bcl-2 family inhibitors. PLoS One 2020; 15: e0240718. https://doi.org/10.1371/journal.pone.0240718

[24] WU ZX, YANG Y, WANG G, WANG JQ, TENG QX et al. Dual TTK/CLK2 inhibitor, CC-671, selectively antagonizes ABCG2-mediated multidrug resistance in lung cancer cells. Cancer Sci 2020; 111: 2872–2882. https://doi.org/10.1111/cas.14505

[25] SALVADOR F, GOMIS RR. CLK2 blockade modulates alternative splicing compromising MYC-driven breast tumors. EMBO Mol Med 2018; 10: e9213. https://doi.org/10.15252/emmm.2018 09213

[26] IWAI K, YAGUCHI M, NISHIMURA K, YAMAMOTO Y, TAMURA T et al. Anti-tumor efficacy of a novel CLK inhibitor via targeting RNA splicing and MYC-dependent vulnerability. EMBO Mol Med 2018; 10: e8289. https://doi.org/10.15252/emmm.201708289

[27] RIGGS JR, NAGY M, ELSNER J, ERDMAN P, CASHION D et al. The Discovery of a Dual TTK Protein Kinase/CDC2-Like Kinase (CLK2) Inhibitor for the Treatment of Triple Negative Breast Cancer Initiated from a Phenotypic Screen. J Med Chem 2017; 60: 8989–9002. https://doi.org/10.1021/acs.jmedchem.7b01223

[28] DESHMUKH V, O'GREEN AL, BOSSARD C, SEO T, LAMANGAN L et al. Modulation of the Wnt pathway through inhibition of CLK2 and DYRK1A by lorecivivint as a novel, potentially disease-modifying approach for knee osteoarthritis treatment. Osteoarthritis Cartilage. 2019; 27: 1347–1360. https://doi.org/10.1016/j.joca.2019.05.006

[29] SABHA M, SIATON BC, HOCHBERG MC. Lorecivivint, an intra-articular potential disease-modifying osteoarthritis drug. Expert Opin Investig Drugs 2020; 29: 1339–1346. https://doi.org/10.1080/13543784.2020.1842357

[30] Tam BY, Chiu K, Chung H, Bossard C, Nguyen JD et al. The CLK inhibitor SM08502 induces anti-tumor activity and reduces Wnt pathway gene expression in gastrointestinal cancer models. Cancer Lett 2020; 473: 186–197. https://doi.org/10.1016/j.canlet.2019.09.009

[31] CHUNG H, CREGER E, SITTS L, CHIU K, MAK CC et al. Sm09419, a novel, small-molecule cdc-like kinase (clk) inhibitor, demonstrates strong inhibition of the wnt signaling pathway and antitumor effects in mantle cell lymphoma models. Blood 2019, 134: 4059. https://doi.org/10.1182/blood-2019-124812

[32] SELLIN JH, UMAR S, XIAO J, MORRIS AP. Increased beta-catenin expression and nuclear translocation accompany cellular hyperproliferation in vivo. Cancer Res 2001; 61: 2899–2906.

https://doi.org/10.4149/neo_2022_220206N138

CDC Like Kinase 2 plays an oncogenic role in colorectal cancer via modulating the Wnt/β-catenin signaling

Hai-Bo ZHOU[1,2], Li YANG[3], Shi-Fang LIU[1], Xin-Hua XU[1], Zhuo CHEN[1], Yun-Xiao LI[1], Jin-Hua YUAN[1,*], Yong-Chang WEI[2,*]

Supplementary Information

Supplementary Table S1. Primers used for RT-PCR assay.

Name	Sequences
CLK2	Forward primer: AATATTTTTACCGGGGTCGC
	Reverse primer: AGCCGCTTAGCTGGTTCATA
GAPDH	Forward primer: CGAGATCCCTCCAAAATCAA
	Reverse primer: GTCTTCTGGGTGGCAGTG
β-catenin	Forward primer: GAGCCTGCCATCTGTGCTCT
	Reverse primer: ACGCAAAGGTGCATGATTTG
c-Myc	Forward primer: GCTGGACCAGATGTATGTCCC
	Reverse primer: ATCATTTCCATGACGGCCTGT
cyclin D1	Forward primer: TCCTCTCCAAAATGCCAGAG
	Reverse primer: GGCGGATTGGAAATGAACTT
MMP7	Forward primer: ATGTGGAGTGCCAGATGTTGC
	Reverse primer: AGCAGTTCCCCATACAACTTTC
CD44	Forward primer: AGCCCATGTTGTAGCAAACC
	Reverse primer: TGAGGTACAGGCCCTCTGAT

Supplementary Table S2. Correlation of CLK2 expression with wnt related genes in CRC.

Symbol Gene	ID	Description	cor	p-value	pstar
AKT1	207	v-akt murine thymoma viral oncogene homolog 1	0.302	1.94E-14	**
AKT2	208	V-akt murine thymoma viral oncogene homolog 2, mRNA	0.379	0	**
AKT3	10000	v-akt murine thymoma viral oncogene homolog 3 (protein kinase B, gamma)	0.008	0.834698919	
ANKRD6	22881	ankyrin repeat domain 6	0.072	0.071305047	
APC	324	adenomatous polyposis coli	0.112	0.005076068	**
APC2	10297	adenomatosis polyposis coli 2	0.245	7.52E-10	**
ARRB1	408	arrestin, beta 1	–0.049	0.220667891	
ARRB2	409	arrestin, beta 2	0.087	0.03004937	*
AXIN1	8312	axin 1	0.335	9.29E-18	**
AXIN2	8313	axin 2	0.084	0.035953306	*
BRD7	29117	bromodomain containing 7	0.154	0.000121433	**
BTRC	8945	beta-transducin repeat containing	0.262	4.27E-11	**
PGEA1	25776	(CBY1) chibby homolog 1 (Drosophila)	–0.066	0.098492265	
CACYBP	27101	calcyclin binding protein	0.089	0.026613974	*
CAMK2A	815	calcium/calmodulin-dependent protein kinase II alpha	0.257	8.84E-11	**
CAMK2B	816	calcium/calmodulin-dependent protein kinase II beta	0.187	2.67E-06	**
CAMK2D	817	calcium/calmodulin-dependent protein kinase II delta	0.055	0.170895028	
CAMK2G	818	calcium/calmodulin-dependent protein kinase II gamma	0.307	7.85E-15	**
CCND1	595	cyclin D1	0.161	5.74E-05	**
CCND2	894	cyclin D2	0.105	0.008625284	**
CCND3	896	Cyclin D3 (CCND3), transcript variant 3, mRNA	0.049	0.225218154	
CDC2	983	cell division cycle 2, G1 to S and G2 to M	–0.030	0.453196678	
CDC25C	995	cell division cycle 25 homolog C (S. pombe)	–0.032	0.431040741	
CDH1	999	cadherin 1, type 1, E-cadherin (epithelial)	0.060	0.133177533	

Supplementary Table S2. ***Continued ...***

Symbol Gene	ID	Description	cor	p-value	pstar
CDX1	1044	caudal type homeobox 1	–0.131	0.001077148	**
CER1	9350	cerberus 1, cysteine knot superfamily, homolog (Xenopus laevis)	0.102	0.010731154	*
CHD8	57680	chromodomain helicase DNA binding protein 8	0.333	1.71E-17	**
CHP	11261	calcium binding protein P22	0.025	0.541039127	
CREBBP	1387	CREB binding protein	0.380	0	**
CSNK1A1	1452	Homo sapiens, clone IMAGE:4769127, mRNA	0.006	0.883657533	
CSNK1D	1453	casein kinase 1, delta	0.341	2.18E-18	**
CSNK1E	1454	casein kinase 1, epsilon	0.449	0	**
CSNK2A1	1457	casein kinase 2, alpha 1 polypeptide	0.051	0.208107603	
CSNK2A2	1459	casein kinase 2, alpha prime polypeptide	0.165	3.78E-05	**
CSNK2B	1460	casein kinase 2, beta polypeptide	0.161	5.74E-05	**
CTBP1	1487	C-terminal binding protein 1	0.333	1.89E-17	**
CTBP2	1488	C-terminal binding protein 2	0.200	5.71E-07	**
CTNNB1	1499	catenin (cadherin-associated protein), beta 1, 88kDa	–0.034	0.402221558	
CTNNBIP1	56998	catenin, beta interacting protein 1	0.082	0.040127351	*
CUL1	8454	cullin 1	0.008	0.844622832	
CXXC4	80319	CXXC finger 4	0.089	0.026559654	*
DAAM1	23002	dishevelled associated activator of morphogenesis 1	0.127	0.001528014	**
DAAM2	23500	dishevelled associated activator of morphogenesis 2	0.028	0.493744287	
DAB2	1601	Differentially expressed protein	0.013	0.749512001	
DACT1	51339	dapper, antagonist of beta-catenin, homolog 1 (Xenopus laevis)	0.067	0.097686912	
CCDC85B	11007	coiled-coil domain containing 85B	–0.014	0.727691336	
DKK1	22943	dickkopf homolog 1 (Xenopus laevis)	0.028	0.488323217	
DKK2	27123	dickkopf homolog 2 (Xenopus laevis)	–0.098	0.014978903	*
DKK3	27122	dickkopf homolog 3 (Xenopus laevis)	–0.107	0.00795153	**
DKK4	27121	dickkopf homolog 4 (Xenopus laevis)	0.040	0.317375768	
DLG1	1739	discs, large homolog 1 (Drosophila)	0.147	0.000232242	**
DLG2	1740	discs, large homolog 2 (Drosophila)	0.037	0.359656268	
DLG4	1742	discs, large homolog 4 (Drosophila)	0.252	2.45E-10	**
DVL1	1855	dishevelled, dsh homolog 1 (Drosophila)	0.293	1.17E-13	**
DVL2	1856	dishevelled, dsh homolog 2 (Drosophila)	0.241	1.40E-09	**
DVL3	1857	dishevelled, dsh homolog 3 (Drosophila)	0.464	0	**
EP300	2033	E1A binding protein p300	0.246	5.67E-10	**
FBXW11	23291	F-box and WD repeat domain containing 11	0.130	0.001238214	**
FBXW2	26190	F-box and WD repeat domain containing 2	0.344	5.58E-19	**
FOSL1	8061	FOS-like antigen 1	0.000	0.993596532	
FRAT1	10023	frequently rearranged in advanced T-cell lymphomas	0.325	1.23E-16	**
FRAT2	23401	frequently rearranged in advanced T-cell lymphomas 2	0.202	4.44E-07	**
FSTL1	11167	follistatin-like 1	–0.094	0.0194112	*
FZD1	8321	frizzled homolog 1 (Drosophila)	0.025	0.539845588	
FZD10	11211	frizzled homolog 10 (Drosophila)	0.010	0.811138638	
FZD2	2535	frizzled homolog 2 (Drosophila)	0.129	0.001346998	**
FZD3	7976	frizzled homolog 3 (Drosophila)	–0.026	0.522709225	
FZD4	8322	frizzled homolog 4 (Drosophila)	0.128	0.001469704	**
FZD5	7855	frizzled homolog 5 (Drosophila)	0.141	0.000450672	**
FZD6	8323	frizzled homolog 6 (Drosophila)	0.101	0.012217139	*
FZD7	8324	frizzled homolog 7 (Drosophila)	0.081	0.04305449	*
FZD8	8325	frizzled homolog 8 (Drosophila)	0.024	0.550174033	
FZD9	8326	frizzled homolog 9 (Drosophila)	0.109	0.006749666	**
GSK3A	2931	glycogen synthase kinase 3 alpha	0.210	1.34E-07	**
GSK3B	2932	glycogen synthase kinase 3 beta	0.190	2.09E-06	**
HDAC1	3065	histone deacetylase 1	0.063	0.118628988	
HIPK2	28996	homeodomain interacting protein kinase 2	0.181	6.09E-06	**

Supplementary Table S2. ***Continued ...***

Symbol Gene	ID	Description	cor	p-value	pstar
JUN	3725	jun oncogene	0.222	2.61E-08	**
RPSA	3921	ribosomal protein SA	–0.002	0.964881	
LDLR	3949	low density lipoprotein receptor	0.063	0.118300299	
LEF1	51176	lymphoid enhancer-binding factor 1	0.066	0.098147051	
LRP1	4035	low density lipoprotein-related protein 1 (alpha-2-macroglobulin receptor)	0.190	2.10E-06	**
LRP5	4041	low density lipoprotein receptor-related protein 5	0.341	1.61E-18	**
LRP6	4040	low density lipoprotein receptor-related protein 6	0.258	7.96E-11	**
MAGI3	260425	membrane associated guanylate kinase, WW and PDZ domain containing 3	0.075	0.061412132	
MAP1B	4131	microtubule-associated protein 1B	0.071	0.077309473	
MAP3K4	4216	mitogen-activated protein kinase kinase kinase 4	0.361	0	**
MAP3K7	6885	mitogen-activated protein kinase kinase kinase 7	0.163	4.56E-05	**
TAB1	10454	TGF-beta activated kinase 1/MAP3K7 binding protein 1	0.223	2.29E-08	**
MAPK10	5602	mitogen-activated protein kinase 10	–0.059	0.144495249	
MAPK8	5599	mitogen-activated protein kinase 8	0.033	0.411646904	
MAPK8IP1	9479	mitogen-activated protein kinase 8 interacting protein 1	0.103	0.010392259	*
MAPK9	5601	mitogen-activated protein kinase 9	0.072	0.071419753	
MARK2	2011	MAP/microtubule affinity-regulating kinase 2	0.282	1.10E-12	**
MMP7	4316	matrix metallopeptidase 7 (matrilysin, uterine)	–0.156	0.000100646	**
MVP	9961	major vault protein	0.114	0.004490841	**
MYC	4609	v-myc myelocytomatosis viral oncogene homolog (avian)	–0.035	0.382173461	
NFAT5	10725	nuclear factor of activated T-cells 5, tonicity-responsive	0.277	2.65E-12	**
NFATC1	4772	nuclear factor of activated T-cells, cytoplasmic, calcineurin-dependent 1	0.090	0.024934033	*
NFATC2	4773	nuclear factor of activated T-cells, cytoplasmic, calcineurin-dependent 2	0.111	0.00567666	**
NFATC3	4775	nuclear factor of activated T-cells, cytoplasmic, calcineurin-dependent 3	0.178	8.22E-06	**
NFATC4	4776	nuclear factor of activated T-cells, cytoplasmic, calcineurin-dependent 4	0.360	0	**
NKD1	85407	naked cuticle homolog 1 (Drosophila)	0.154	0.000121246	**
NKD2	85409	naked cuticle homolog 2 (Drosophila)	0.223	2.09E-08	**
NLK	51701	nemo-like kinase	0.098	0.01456143	*
NR5A1	2516	nuclear receptor subfamily 5, group A, member 1	0.197	8.05E-07	**
PAFAH1B1	5048	platelet-activating factor acetylhydrolase, isoform Ib, alpha subunit 45kDa	0.096	0.01647333	*
PAX2	5076	paired box 2	0.137	0.000611769	**
PIAS4	51588	protein inhibitor of activated STAT, 4	0.297	5.85E-14	**
PIN1	5300	peptidylprolyl cis/trans isomerase, NIMA-interacting 1	0.019	0.640491971	
PLAU	5328	plasminogen activator, urokinase	–0.022	0.589770109	
PLCB1	23236	phospholipase C, beta 1 (phosphoinositide-specific)	0.026	0.522153137	
PLCB2	5330	phospholipase C, beta 2	0.297	5.65E-14	**
PLCB3	5331	phospholipase C, beta 3 (phosphatidylinositol-specific)	0.306	8.76E-15	**
PLCB4	5332	phospholipase C, beta 4	–0.032	0.430422486	
PORCN	64840	porcupine homolog (Drosophila)	0.174	1.42E-05	**
PPARD	5467	peroxisome proliferator-activated receptor delta	0.242	1.22E-09	**
PPP2CA	5515	protein phosphatase 2 (formerly 2A), catalytic subunit, alpha isoform	–0.178	8.79E-06	**
PPP2CB	5516	protein phosphatase 2 (formerly 2A), catalytic subunit, beta isoform	–0.111	0.005871183	**
PPP2R1A	5518	protein phosphatase 2 (formerly 2A), regulatory subunit A, alpha isoform	0.211	1.29E-07	**
PPP2R1B	5519	protein phosphatase 2 (formerly 2A), regulatory subunit A, beta isoform	0.042	0.297026399	
PPP2R2A	5520	protein phosphatase 2 (formerly 2A), regulatory subunit B, alpha isoform	–0.089	0.026778459	*
PPP2R2B	5521	protein phosphatase 2 (formerly 2A), regulatory subunit B, beta isoform	–0.023	0.563622325	
PPP2R2C	5522	protein phosphatase 2 (formerly 2A), regulatory subunit B, gamma isoform	0.116	0.003688203	**
PPP2R5B	5526	protein phosphatase 2, regulatory subunit B', beta isoform	0.131	0.001116141	**
PPP2R5C	5527	protein phosphatase 2, regulatory subunit B', gamma isoform	0.063	0.114233607	
PPP2R5E	5529	protein phosphatase 2, regulatory subunit B', epsilon isoform	0.039	0.336564837	
PPP3CA	5530	protein phosphatase 3 (formerly 2B), catalytic subunit, alpha isoform	0.040	0.319849738	
PPP3CB	5532	protein phosphatase 3 (formerly 2B), catalytic subunit, beta isoform	–0.031	0.441184453	
PPP3CC	5533	protein phosphatase 3 (formerly 2B), catalytic subunit, gamma isoform	–0.082	0.041099984	*

Supplementary Table S2. ***Continued ...***

Symbol Gene	ID	Description	cor	p-value	pstar
PPP3R1	5534	protein phosphatase 3, regulatory subunit B, alpha	–0.029	0.467116469	
PPP3R2	5535	protein phosphatase 3 (formerly 2B), regulatory subunit B, beta isoform	0.069	0.087019426	
PRICKLE1	144165	prickle homolog 1 (Drosophila)	0.003	0.933286722	
PRICKLE2	166336	prickle homolog 2 (Drosophila)	0.049	0.225124227	
PRKACA	5566	protein kinase, cAMP-dependent, catalytic, alpha	0.129	0.001246101	**
PRKACB	5567	protein kinase, cAMP-dependent, catalytic, beta	–0.117	0.003532838	**
PRKACG	5568	protein kinase, cAMP-dependent, catalytic, gamma	0.035	0.378719062	
PRKCA	5578	protein kinase C, alpha	0.166	3.54E-05	**
PRKCB1	5579	protein kinase C, beta 1	–0.017	0.668764013	
PRKCD	5580	protein kinase C, delta	0.233	5.20E-09	**
PRKCE	5581	protein kinase C, epsilon	0.144	0.000341895	**
PRKCG	5582	protein kinase C, gamma	0.184	3.96E-06	**
PRKCH	5583	protein kinase C, eta	0.113	0.005014574	**
PRKCI	5584	protein kinase C, iota	0.027	0.507000178	
PRKCQ	5588	protein kinase C, theta	0.068	0.088342396	
PRKCZ	5590	Protein kinase C zeta	0.113	0.004862865	**
PRKD1	5587	protein kinase D1	–0.019	0.640335247	
PRKX	5613	protein kinase, X-linked	0.097	0.015769586	*
PRKY	5616	protein kinase, Y-linked			
PSEN1	5663	presenilin 1	0.034	0.398198017	
PTPRA	5786	protein tyrosine phosphatase, receptor type, A	0.083	0.039874761	*
RAC1	5879	MRNA, clone: PO2ST9	–0.079	0.050454217	
RAC2	5880	ras-related C3 botulinum toxin substrate 2	0.063	0.117326729	
RAC3	5881	ras-related C3 botulinum toxin substrate 3	0.213	9.85E-08	**
RBX1	9978	ring-box 1	–0.237	2.60E-09	**
RHOA	387	ras homolog gene family, member A	–0.201	4.64E-07	**
ROCK1	6093	Rho-associated, coiled-coil containing protein kinase 1	0.108	0.006973579	**
ROCK2	9475	Rho-associated, coiled-coil containing protein kinase 2	0.123	0.002133893	**
ROR2	4920	receptor tyrosine kinase-like orphan receptor 2	0.005	0.906952562	
RUNX2	860	runt-related transcription factor 2	0.080	0.045587745	*
RUVBL1	8607	RuvB-like 1 (E. coli)	0.098	0.014809137	*
SALL1	6299	sal-like 1 (Drosophila)	–0.037	0.362089041	
SENP2	59343	SUMO1/sentrin/SMT3 specific peptidase 2	0.159	6.94E-05	**
SFRP1	6422	secreted frizzled-related protein 1	–0.027	0.505670434	
SFRP2	6423	secreted frizzled-related protein 2	–0.036	0.36993262	
SFRP4	6424	secreted frizzled-related protein 4	–0.079	0.049512828	*
SFRP5	6425	secreted frizzled-related protein 5	0.011	0.784565239	
SIAH1	6477	seven in absentia homolog 1 (Drosophila)	0.057	0.153435217	
SKP1A	6500	S-phase kinase-associated			
SMAD2	4087	SMAD family member 2	0.037	0.358224896	
SMAD3	4088	SMAD family member 3	0.256	1.11E-10	**
SMAD4	4089	CDNA FLJ59261 complete cds	0.053	0.191214654	
SOX1	6656	SRY (sex determining region Y)-box 1	0.006	0.87520977	
SOX17	64321	SRY (sex determining region Y)-box 17	0.030	0.450772828	
TAX1BP3	30851	Tax1 (human T-cell leukemia virus type I) binding protein 3	–0.042	0.292964171	
TBL1X	6907	transducin (beta)-like 1X-linked	0.143	0.000351579	**
TBL1XR1	79718	transducin (beta)-like 1 X-linked receptor 1	0.084	0.037656471	*
TBL1Y	90665	transducin (beta)-like 1Y-linked	–0.021	0.607790303	
TBP	6908	TATA box binding protein	0.190	2.04E-06	**
TCF1	6927	ranscription factor 1	0.272	6.96E-12	**
TCF3	6929	transcription factor 3 (E2A immunoglobulin enhancer binding factors E12/E47)	0.329	4.47E-17	**
TCF4	6925	transcription factor 4	–0.054	0.175918987	
TCF7	6932	transcription factor 7 (T-cell specific, HMG-box)	0.075	0.062782967	

Supplementary Table S2. ***Continued ...***

Symbol Gene	ID	Description	cor	p-value	pstar
TCF7L1	83439	transcription factor 7-like 1 (T-cell specific, HMG-box)	0.161	5.90E-05	**
TCF7L2	6934	transcription factor 7-like 2 (T-cell specific, HMG-box)	0.162	5.46E-05	**
TFAP2A	7020	transcription factor AP-2 alpha (activating enhancer binding protein 2 alpha)	0.092	0.02134755	*
TLE1	7088	transducin-like enhancer of split 1 (E(sp1) homolog, Drosophila)	0.243	9.21E-10	**
TP53	7157	tumor protein p53	0.112	0.005436863	**
TSHB	7252	thyroid stimulating hormone, beta	–0.051	0.207534921	
VANGL1	81839	vang-like 1 (van gogh, Drosophila)	0.073	0.069621401	
VANGL2	57216	vang-like 2 (van gogh, Drosophila)	0.227	1.15E-08	**
WIF1	11197	WNT inhibitory factor 1	0.074	0.064095746	
WNT1	7471	wingless-type MMTV integration site family, member 1	0.085	0.034871867	*
WNT10A	80326	wingless-type MMTV integration site family, member 10A	0.011	0.781928767	
WNT10B	7480	wingless-type MMTV integration site family, member 10B	0.219	3.36E-08	**
WNT11	7481	wingless-type MMTV integration site family, member 11	0.092	0.022181409	*
WNT16	51384	wingless-type MMTV integration site family, member 16	0.071	0.077895676	
WNT2	7472	wingless-type MMTV integration site family member 2	–0.118	0.003148864	**
WNT2B	7482	wingless-type MMTV integration site family, member 2B	0.118	0.003325647	**
WNT3	7473	wingless-type MMTV integration site family, member 3	0.189	2.11E-06	**
WNT4	54361	wingless-type MMTV integration site family, member 4	0.020	0.61744758	
WNT5A	7474	wingless-type MMTV integration site family, member 5A	–0.123	0.002226835	**
WNT5B	81029	wingless-type MMTV integration site family, member 5B	0.065	0.103808285	
WNT6	7475	wingless-type MMTV integration site family, member 6	0.119	0.00296215	**
WNT7A	7476	wingless-type MMTV integration site family, member 7A	0.062	0.123363819	
WNT7B	7477	wingless-type MMTV integration site family, member 7B	0.073	0.070649423	
WNT8A	7478	wingless-type MMTV integration site family, member 8A			
WNT8B	7479	wingless-type MMTV integration site family, member 8B	0.180	6.68E-06	**
WNT9A	7483	wingless-type MMTV integration site family, member 9A	0.138	0.000602536	**
WNT9B	7484	wingless-type MMTV integration site family, member 9B	–0.033	0.409143024	